Geomatics, Natural Hazards and Risk, 2014
http://dx.doi.org/10.1080/19475705.2014.983187

Estimation of present-day inter-seismic deformation in Kopili fault zone of north-east India using GPS measurements

PRAKASH BARMAN†, JAGAT DWIPENDRA RAY†, ASHOK KUMAR*†, J.D. CHOWDHURY‡ and KAHSYAP MAHANTA‡

†Department of Physics, Tezpur University, Tezpur 784028, India
‡Department of Geography, Jagiroad College, Gauhati University, Jagiroad 782410, India

(*Received 28 October 2013; accepted 13 October 2014*)

Current study reports the present-day inter-seismic deformation of Kopili fault zone of north-east India and slip rate estimate of Kopili fault using five epochs of global positioning system (GPS) data collected from seven campaigns and five permanent sites. The rate of baseline length change of the GPS sites across the Kopili fault indicates ~2.0 mm/yr E–W convergence across the fault. The fault parallel GPS site velocities clearly indicate dextral slip of the Kopili fault. The fault normal velocities show convergence across the Kopili fault, suggesting it to be a transpressional fault. The fault parallel velocities are inverted for fault slip and locking depth using an elastic dislocation model. The first-order, best-fit elastic dislocation model suggest average right lateral slip of 2.62 ± 0.79 mm/yr and a shallow locking depth (3 ± 2 km) of the Kopili Fault. The slip of the Kopili fault is contributing to seismic moment accumulation (~70.74×10^{15} Nm/yr), sufficient to drive possible future earthquakes (Mw ≥ 5.17).

1. Introduction

The north-east India and adjoining regions lying between latitude 22°–29° N and longitude 88°–98° E having an area of roughly 800,000 km^2 exhibit a complex tectonic framework (figure 1). The north-east India is seismically highly active due to the presence of the eastern Himalayan collision belt to the north and nearly N–S trending Burmese arc to the east and southeast (figure 2). The intra-plate deformation in the presence of these two inter-plate tectonic elements is very complex. The ~2500 km Himalayan collision belt is the result of ongoing thrusting of Indian plate towards Eurasian plates, resulting the rising Himalayas. The Himalayan collision belt extending from Nanga Parbat syntaxis in Pakistan to Namche Barwa syntaxis in Tibet is almost a perfect arc (Bendick et al. 2001) and the convergence across it is considered to be arc normal (Mukul et al. 2010 and references therein). This convergence results in the uplift of Tibetan plateau and crustal shortening and thickening across Himalayan thrust belt (DeCelles et al. 2002). The current rate of Indo-Eurasia convergence measured using global positioning system (GPS) in the north-east India region, across the eastern Arunachal Himalaya, is ~15 mm/yr and is distributed between the lesser as well as higher and Tethyan Himalayas (Jade et al. 2007). The Burmese arc also known as the Indo-Burman fold and thrust belt (IBFTB) is an

*Corresponding author. Email: ask@tezu.ernet.in

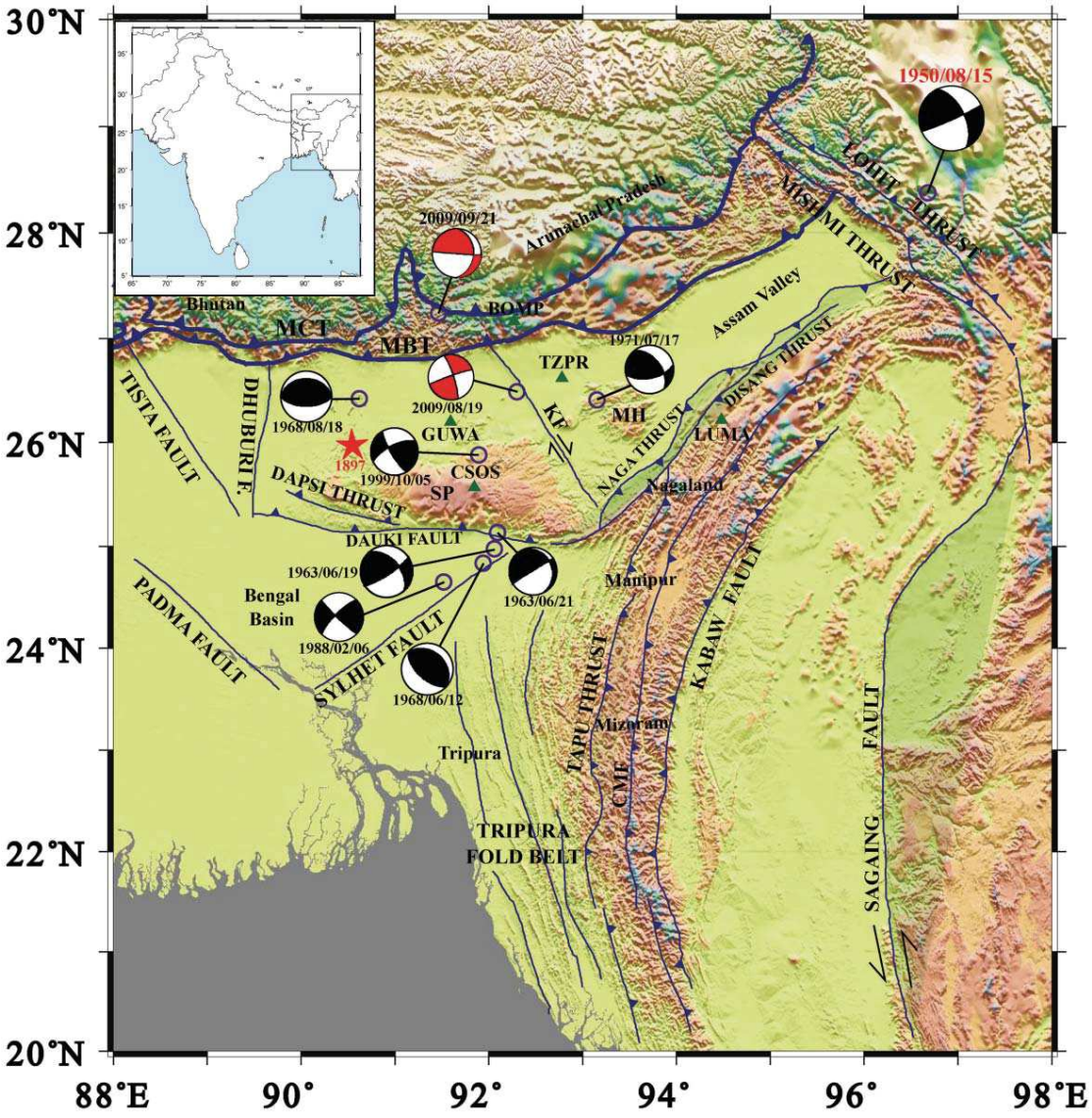

Figure 1. Map showing major tectonic feature of the study region. The focal mechanism solutions of the two recent 2009 earthquakes (shown in red) are taken from Kayal et al. 2012. The focal mechanism for 1999 event is taken from HRVD catalogue and rest focal mechanism are from Chen and Molnar (1990). To view this figure in colour, please see the online version of the journal.
Note: Abbreviations: MCT – main central thrust, MBT – main boundary thrust, KF – Kopili fault, CMF –Churachandpur Mao fault, SP-Shillong plateau, MH-Mikir hills.

elongated crescent-shaped zone extending from Mishmi hills to the Bay of Bengal in NE–SW, NNE–SSW and N–S directions where the Indian plate subducts under Burmese micro-plate and shows very complex deformation. Western IBFTB is segmented into N–S blocks along the E–W transverse zones exhibiting dextral slip between Nagaland salient and Manipur recess and sinistral slip between Manipur recess and Tripura–Mizoram salient (Jade et al. 2007). Towards the east of IBFTB, the India–Sunda relative plate motion of about 36 mm/year is partitioned between the Churachandpur–Mao fault through dextral strike-slip of 16 mm/year (about 43%) and the remaining motion (~20 mm/year) is accommodated at Sagaing fault through dextral strike-slip motion (Kundu & Gahalaut 2013). The NW–SE oblique Mishmi hills thrust front, also known as Assam syntaxis, is the junction where

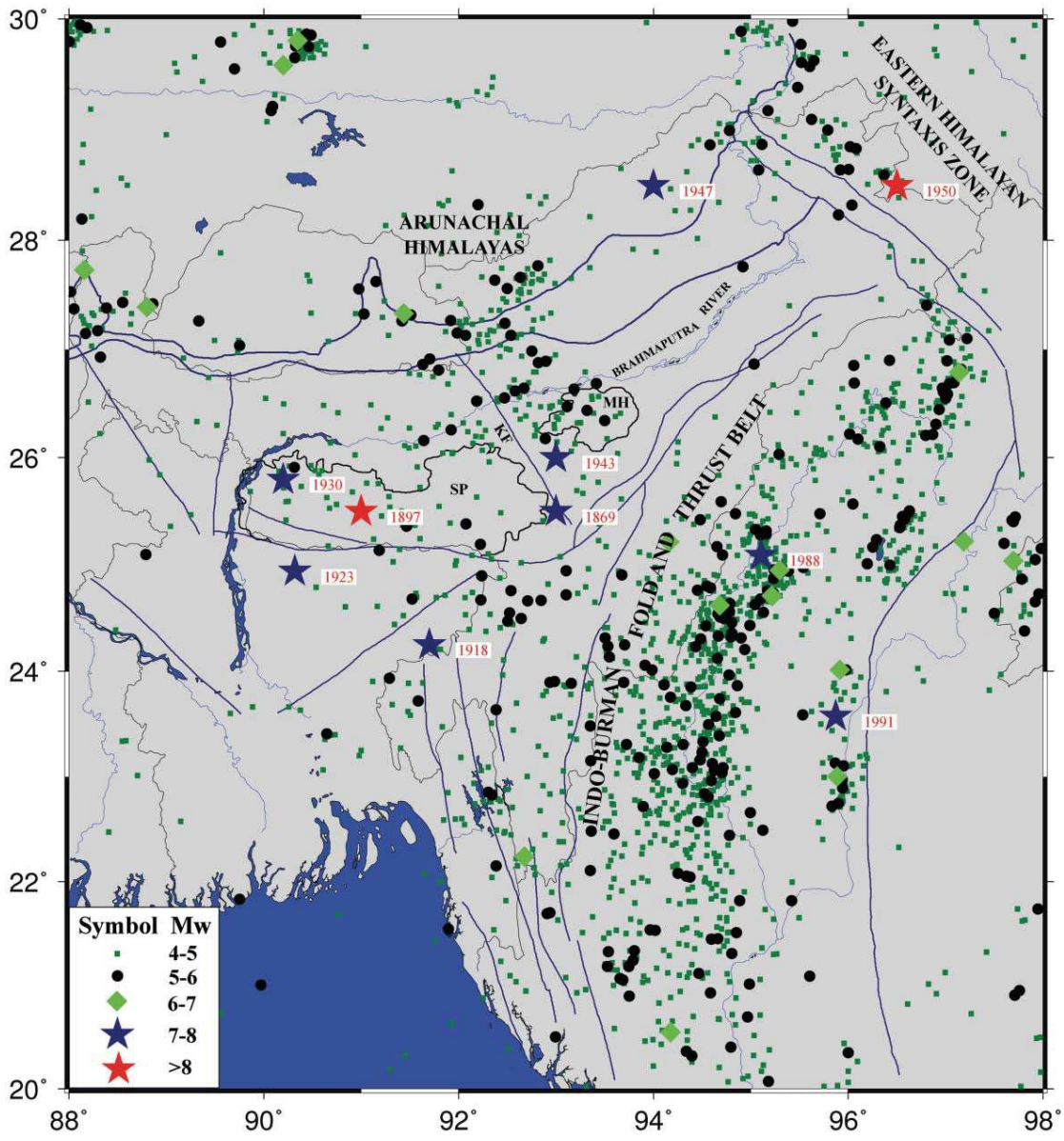

Figure 2. Map showing earthquake distribution in the north-east India region. The earthquake data ($M_w > 4$) are from USGS global earthquake catalogue. The historical earthquake data are from Dasgupta 2011. Abbreviations and fault details are same as in Figure 1 and are omitted for the sake of clarity.

Himalayan collision belt and Indo-Burmese arc converge and was the site for 1950 great Assam earthquake. The syntaxis zone is seismically more active as compared to the Himalayan collision zone (Banerjee et al. 2008).

Juxtaposed between the Himalayan collision belt and Indo-Burmese arc lies the Assam valley with the intra-plate elements, the elevated Shillong plateau and its north-eastern extension in the Mikir Hills. Shillong plateau is a part of the Indian shield (Evans 1964) and exhibits similar seismic characteristic as the Indian shield (Mitra et al. 2005). Geologically, Shillong plateau comprises of rocks from the oldest Precambrian gneissic complex to the recent alluvium formations. Approximately, 1.5–3.5 mm/yr of the present-day total N–S convergence in the eastern Himalaya is accommodated in Shillong plateau (Mukul et al. 2010). The 1897 great Shillong earthquake (Ms 8.7) (Oldham 1899) occurred at western edge of the Shillong plateau.

Shillong plateau is detached from Bengal basin in south by the E–W trending north dipping reverse Dauki fault (Bilham & England 2001). In the west of Shillong plateau lies the north dipping NW–SE trending Dapsi thrust which is western extension of Dauki fault (Kayal et al. 2012). The Brahmaputra River running E–W along Assam valley separates Shillong plateau from the Himalayas to the north, which is termed as the Brahmaputra fault (Nandy 2001) (figure 2). The Shillong plateau is separated in the east from Mikir hills by the NW–SE trending Kopili fault, which is a major active fault in the Assam valley (Nandy 2001). The Shillong plateau, Mikir Hills and the Kopili fault are the main intra-plate seismogenic zones of the study area.

The Kopili fault is mapped as about 300 km long and 50 km wide lineament extending from western part of Manipur up to tri-junction of Bhutan, Arunachal Pradesh and Assam reaching the MBT system (Nandy 2001) (figure 1). The southern end of the Kopili fault cuts across the Naga thrust (Dasgupta & Nandy 1982). Kopili fault was identified as a lineament from Landsat 1 and 2 photo format MSS imagery, generated by NASA (Nandy 1980, 1981). Kopili lineament was later identified as Kopili fault (Dasgupta & Nandy 1982) by studying earthquake hypocentre distribution. Through the study of the Landsat imagery, the number of other major active faults of the north-east India region were identified, viz. Bomdila, Jamuna, Tista, Dudhnai, Sylhet, Gumti, Mat faults and the Siang fracture zones (Nandy 1980, 1981; Dasgupta & Nandy 1982; Dasgupta et al. 1987). Micro-earthquake studies, *b*-value and fractal dimension maps revealed that the Kopili fault is transverse to Himalayan thrust system and is seismically very active (Kayal et al. 2012; Bhattacharya et al. 2002). The presence of springs at the contact of different rock units, folding and interfering deformation in Quaternary sediments, shifting of river channel, river cut off channels, break in slope, etc. are observed in the Kopili gap and suggest it to be a deforming zone (Chowdhury et al. 2005). The 1869 Cacher earthquake (Mw = 7.7) is reported to occur at the south-eastern end of the Kopili fault causing severe damage in the NE India region (Nandy 2001) (figure 2). The 1943 Assam valley earthquake (Mw = 7.2) occurred at the centre of the Kopili fault zone (Kayal et al. 2012). Published fault plane solutions of the recent Bhutan Himalaya earthquake (Mw = 6.3) on 21 September 2009 and the Assam valley earthquake (Mw = 5.1) on 19 August 2009 infers them to originate at the Kopili fault region (Kayal et al. 2010). Bhattacharya et al. (2008) estimated three-dimensional (3D) P-wave velocity (Vp) structure of the north-east India and estimated that the Kopili fault system extends from 20 to 30 km depth and there is a high Vp structure below Mikir Hills at a depth of 40 km. They infer the possibility of stress concentration for high seismic activity along Kopili fault, particularly at the southern fault end. The fault plane solutions of the earthquakes occurring in Kopili fault region indicates that Kopili fault dips towards north-east ($\sim 61^{o}$) and is transverse to MCT (Kayal et al. 2012). Mahesh et al. (2012) using GPS-geodetic technique, observed 3.0 $\pm$ 1.5 mm/yr difference in north velocity component between Guwahati and Tezpur situated on the opposite sides of the Kopili fault. This observation was the first GPS-measured geodetic indication of dextral motion on the Kopili fault. Recently, Vernant et al. (2014) reported that Assam valley is fragmented along Kopili fault into two distinct blocks. The Shillong block between longitudes 89° and 93° E rotating clockwise at 1.15°/M yr and the Assam block from 93.5° to 97° E rotating at $\approx$1.13°/M yr resulting in 2–3 mm/yr dextral slip in Kopili fault. In the current work, we investigate further the neotectonics of the Kopili fault using high precision GPS data collected from four campaign sites across the fault and estimate its current rate of slip and the associated seismic hazard implications.

2. Data and methodology

GPS measurements were made at seven sites in campaign mode for five epochs from 2006 to 2012. Three to four consecutive days of GPS measurements in 24-hr session were collected from each campaign site for each epoch. Data containing less than 12 hr of phase observations were omitted from processing. Data from five continuously running GPS permanent stations, viz. Tezpur (TZPR), Guwahati IMD (GUWA), Shillong (CSOS), Lumami (LUMA) and Bomdila (BOMP) were included in processing for the entire period of 2006–2012. To tie the local reference frame with the global reference frame, nine IGS sites (Dow et al. 2009) BAN2, HYDE, IISC, KIT3, KUNM, LHAZ, POL2, SELE and WUHN were processed along with the campaign and permanent site data. The permanent stations were equipped with Zephyr geodetic antennae with Trimble 5700 receivers mounted on concrete pillars on granite bedrocks. Campaign sites were equipped with Zephyr geodetic antennae and Leica Geosystem 500/Trimble 5700 and are marked with 2–3 mm drilled hole over the bedrock exposure for the subsequent reoccupation.

The phase processing of the GPS data was accomplished using GAMIT/GLOBK version 10.4 (Herring et al. 2010a, 2010b). The loosely constrained full covariance solutions from GAMIT were combined for site position repeatability and rate using GLOBK. Velocity field estimates and time series were estimated in ITRF08 (Altamimi et al. 2011) by stabilizing stable IGS and permanent sites using GLORG. The site velocities in India-fixed reference frame were calculated using the Euler rotation pole of the stable Indian plate ($51.4 \pm .007^{o}$ N, 8.9 ± 0.8^{o} E, Angular velocity: 0.539 ± 0.002^{o}/Ma) reported by Mahesh et al. (2012). The program GLORG, defines the reference frame by applying generalized constraints on frame defining site by minimizing their adjustment of coordinates by estimating Helmert parameters (translation, rotation and scale) (Herring et al. 2010a, 2010b). The long period noises that affects the velocity estimates of sites with >100 position estimates are accounted for by adding random walk noise for each velocity components determined using "Realistic sigma" algorithm described by Herring (2003).

3. Results and discussions

The site velocities estimated in ITRF2008 and India-fixed reference are tabulated in table 1 and illustrated in figures 3 and 4. The IGS sites have average north, east and up (NEU) root mean square (rms) scatters of 1.63, 1.79 and 9.45 mm, respectively. The average NEU rms (root mean square) scatters for the permanent GPS sites are 2.3, 2.5 and 10.6 mm and that for the campaign sites are 3.38, 3.75 and 16.62 mm, respectively. These values are within the acceptable limit for continuous sites (maximum 3 mm) and campaign sites (maximum 5 mm) considering the number of available days of observations. The Indian stable block IGS sites HYDE and IISC have average velocity of ~54 mm/yr towards NE which is Indian absolute plate motion in ITRF2008 calculated in current processing (figure 3). LHAZ in Tibetan-Himalaya has velocity ~49 mm/yr in ENE direction. In the East, the IGS site KUNM has velocity ~36 mm/yr in SE direction. These observations are consistent with the published rates in ITRF2008 (e.g. Mahesh et al. 2012).

3.1. Deformation study using baseline convergence rate

In a GPS network solution, baseline lengths are most accurately estimated and the errors in the baselines are free from the error associated with the realization of the

Table 1. Site velocities estimated in ITRF2008 and India-fixed reference frame.

Site	Site code	Long. (Deg)	Lat. (Deg)	ITRF08 velocities (mm/yr)		India-fixed velocities (mm/yr)		σE (mm/yr)	σN (mm/yr)	Rho
				E-rate	*N*-rate	*E*-rate	*N*-rate			
Bura Mayong	BURA	92.01	26.25	39.36	28.84	−0.77	−8.3	0.59	0.54	−0.065
Jagiroad	JAGI	92.20	26.12	39.65	28.44	−0.59	−8.71	0.65	0.61	0.01
Kampur	KAMP	92.65	26.16	39.9	28.94	−0.45	−8.25	0.89	0.78	0.016
Kheroni	KHER	92.86	25.81	40.34	28.68	−0.21	−8.52	0.39	0.35	0.005
Panimura	PANI	92.83	25.72	38.18	29.48	−2.4	−7.72	0.37	0.35	−0.009
Raja Ali	RAJA	92.63	26.07	38.64	29.08	−1.74	−8.11	0.4	0.39	0.056
Umrangsho	UMRA	92.73	25.53	38.21	27.61	−2.42	−9.58	0.51	0.48	0.007
Bomdila	BOMP	92.41	27.27	41.93	19.54	2.13	−17.63	0.18	0.56	−0.001
Shillong	CSOS	91.86	25.57	39.88	30.84	−0.49	−6.29	0.71	0.45	0.018
Guwahati	GUWA	91.59	26.10	40.56	29.99	0.49	−7.12	0.94	0.69	0.003
Lumami	LUMA	94.48	26.22	37.86	22.86	−2.98	−14.44	0.36	0.56	0.001
Tezpur	TZPR	92.78	26.62	40.3	27.03	0.11	−10.17	0.09	0.09	0.001
Bangalore	BAN2	77.51	13.03	42.06	35.92	−0.59	1.07	0.07	0.07	0.004
Hyderabad	HYDE	78.55	17.42	39.98	34.41	−0.92	−0.68	0.22	0.42	0.001
Bangalore	IISC	77.57	13.02	41.86	35.69	−0.8	0.83	0.07	0.07	0.004
Kitab	KIT3	66.89	39.13	29.65	3.16	5.67	−28.54	0.26	0.27	0.002
Kunming	KUNM	102.80	25.03	31.09	−17.51	−12.51	−54.83	0.04	0.04	0.008
Lhasa	LHAZ	91.10	29.66	46.96	15.21	8.66	−21.85	0.36	0.17	0.001
Kyrgyzstan	POL2	74.69	42.68	26.77	4.69	2.58	−29.4	0.07	0.06	0.011
Kazakhstan	SELE	77.02	43.18	28.73	3.88	3.97	−30.8	0.07	0.07	−0.016
China	WUHN	114.36	30.53	31.87	−11.4	−13.61	−47.45	0.31	0.2	0.001

reference frame. Hence, we consider the rate of baseline length change of continuous GPS sites TZPR (east of Kopili fault), CSOS and GUWA (west of Kopili fault) with respect to the other continuous GPS sites (figure 5). All the north-eastern sites are converging with respect to stable Indian peninsular site IISC, and are obviously due to resistances offered by the surrounding inter-plate tectonic elements (Eastern Himalayan collision belt, Assam syntaxis and Indo-Burman subduction zone) to the dominant Indian plate motion. The rates of baseline length change between IISC to GUWA and CSOS are -4.61 ± 0.94 and -3.65 ± 0.70 mm/yr, respectively, which implies negligible deformation between Shillong plateau and Guwahati. The IISC to TZPR baseline, east of the Kopili fault, converges at the rate of 6.30 ± 0.25 mm/yr. These convergence rates of IISC to CSOS, GUWA and TZPR are consistent with the 4–7 mm/yr convergence reported elsewhere (Jade et al. 2007; Banerjee et al. 2008). The baseline converging rates, east and west to Kopili fault with respect to IISC suggests ~2.1 mm/yr of E–W convergence across the Kopili fault. These observations also indicate that the Assam valley is deforming along Kopili fault, since it is the only known fault separating the sites in east and west. The baselines GUWA-TZPR and CSOS-TZPR which are almost normal to the strike of the Kopili fault are converging at the rate of 1.64 ± 0.91 and 2.55 ± 0.58 mm/yr, respectively. This

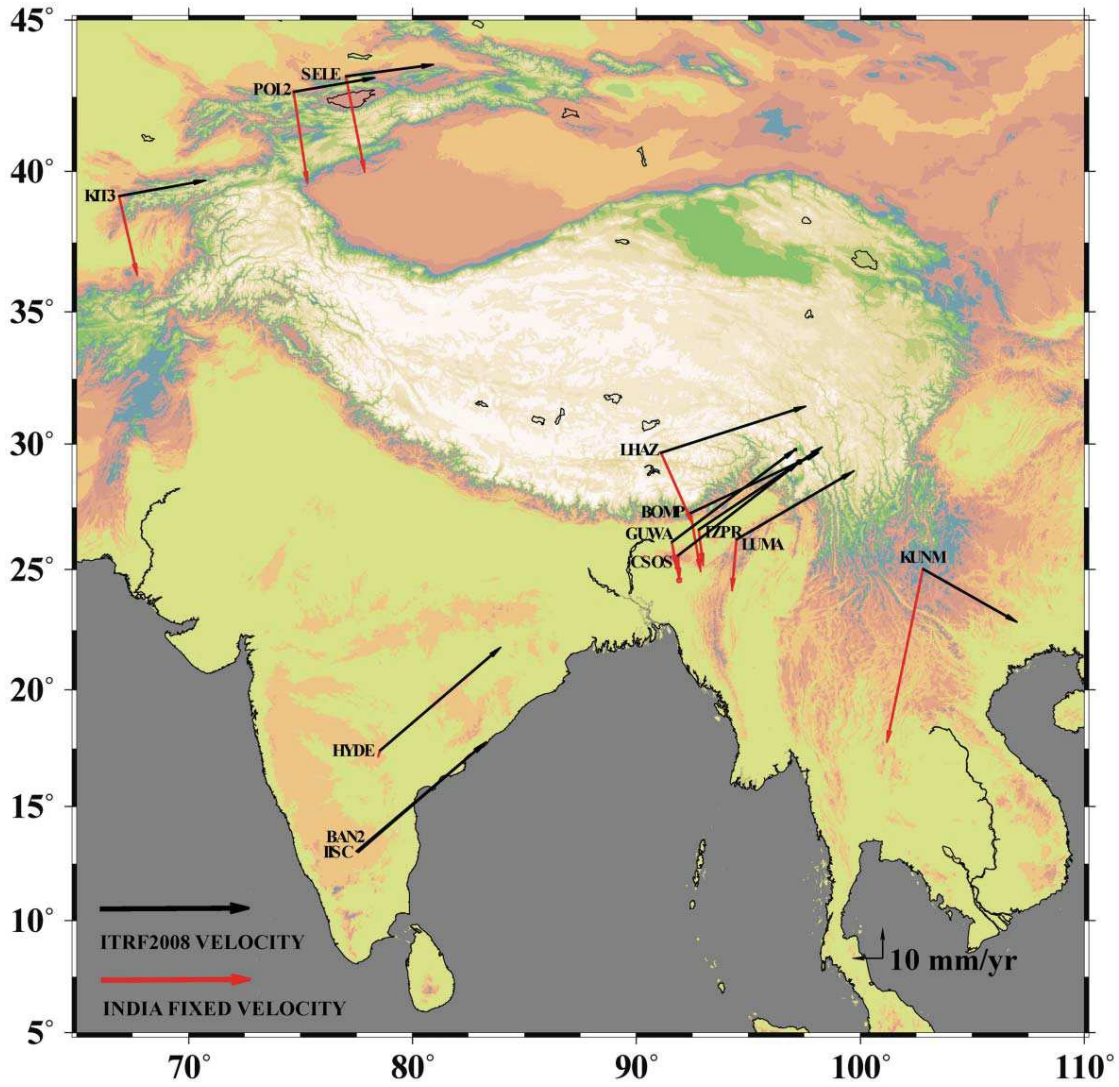

Figure 3. ITRF2008 and India-fixed velocities of IGS and permanent GPS sites of current study.

observation clearly implies that, there is ~2.1 mm/yr E–W compression across the Kopili fault.

From the convergence rate of baselines of GUWA, CSOS and TZPR with respect to BOMP (figure 5), higher convergence rate in the BOMP-CSOS baseline is observed. The convergence rate of BOMP-CSOS baseline includes components of both E–W compression and dextral slip of the Kopili fault, in addition to the N–S convergence due to Indo-Eurasia plate collision. However, these observations are not conclusive since BOMP is situated at an asymmetrical location to the fault (east of the fault) and located on the footwall of MCT which is a different active deforming zone.

The baseline convergence rate of TZPR, GUWA and CSOS with respect to LUMA suggests gradually increasing compression from north to south across Assam valley and Shillong plateau. This observation cannot be attributed solely to the Kopili fault, as the western IBFTB is itself segmented into N–S blocks along the E–W transverse zones as pointed out by Jade et al. (2007). These observations exhibit the complex deformation prevailing in the north-eastern India.

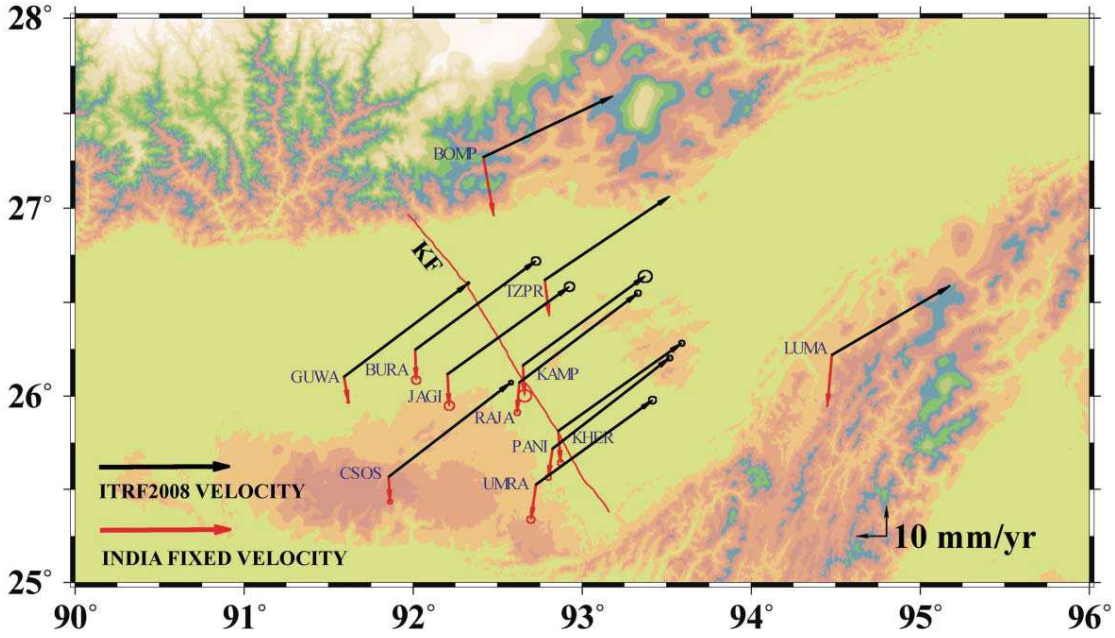

Figure 4. ITRF2008 and India-fixed velocities of campaign and permanent GPS sites of current study. Error ellipses signifies 95% confidence level of formal uncertainties.

3.2. Deformation study using site kinematics

The sites in Assam valley move with an average velocity of 9−10 mm/yr towards the south of south-east in India-fixed reference frame (figure 4). To access the local deformation across the Kopili fault, we find the relative velocities of the neighbouring sites with respect to TZPR (figure 6 and table 2). The sites show 1.7−3.9 mm/yr

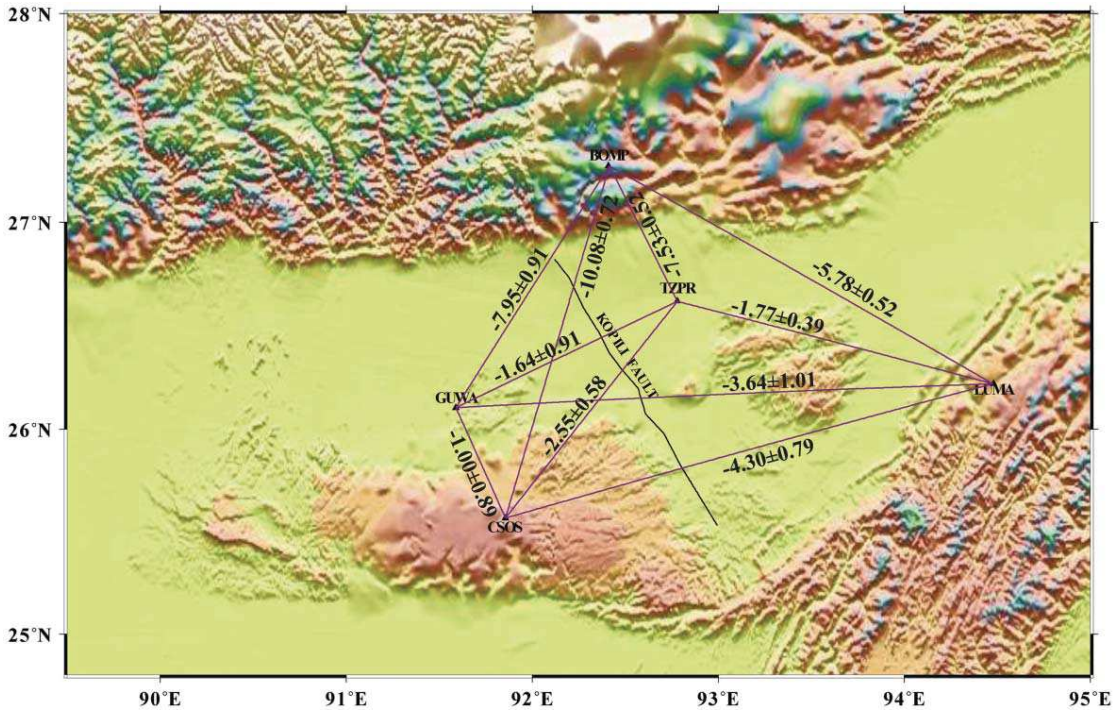

Figure 5. Baseline convergence rate (in mm/yr) among permanent GPS sites of the study area. IISC-GUWA, IISC-CSOS and IISC-TZPR baselines converge at the rate of 4.61 ± 0.94, 3.65 ± 0.70 and 6.30 ± 0.25 mm/yr (not shown in the figure).

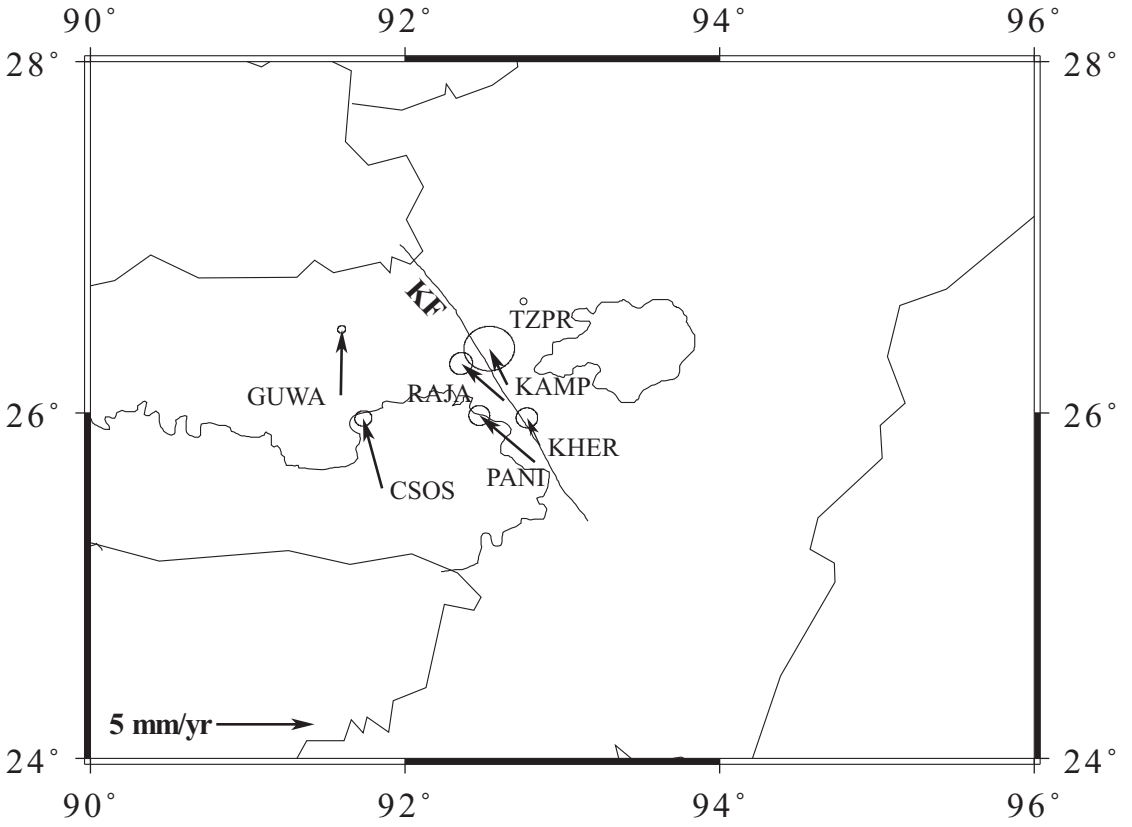

Figure 6. Relative velocities around Kopili fault with respect to TZPR permanent GPS stations depicting sense of faulting on Kopili fault. Error ellipses show 95% confidence interval. Note: Abbreviations: KF – Kopili fault.

NNW directed velocities relative to TZPR. The sites west of the fault (CSOS, GUWA, RAJA and PANI) shows ~3.3 mm/yr NNW velocity compared to ~1.8 mm/yr of the sites east of the fault (KAMP and KHER). The difference of the magnitudes of the TZPR-fixed site velocities either side of the fault indicates right lateral faulting of the Kopili fault. The India-fixed velocities are resolved along strike-parallel and strike-normal directions (figure 7) to access further the relative sense of motion of the sites across the fault. The strike-parallel site motion across the fault indicates right lateral faulting of the fault. The strike-normal velocity components of the permanent sites TZPR, GUWA and CSOS which have long period data as well as away from the deforming zone suggest average E–W compression of ~2 mm/yr.

Table 2. Velocities of GPS stations relative to TZPR GPS site.

Site	*E* (mm/yr)	*N* (mm/yr)	Resultant (mm/yr)
TZPR	0	0	0
KAMP	-0.56 ± 0.80	1.92 ± 0.69	2.00 ± 0.70
KHER	-0.32 ± 0.30	1.65 ± 0.26	1.68 ± 0.26
GUWA	0.38 ± 0.85	3.05 ± 0.60	3.07 ± 0.60
CSOS	-0.60 ± 0.62	3.88 ± 0.36	3.93 ± 0.37
PANI	-2.51 ± 0.28	2.45 ± 0.26	3.51 ± 0.27
RAJA	-1.85 ± 0.31	2.06 ± 0.30	2.77 ± 0.30

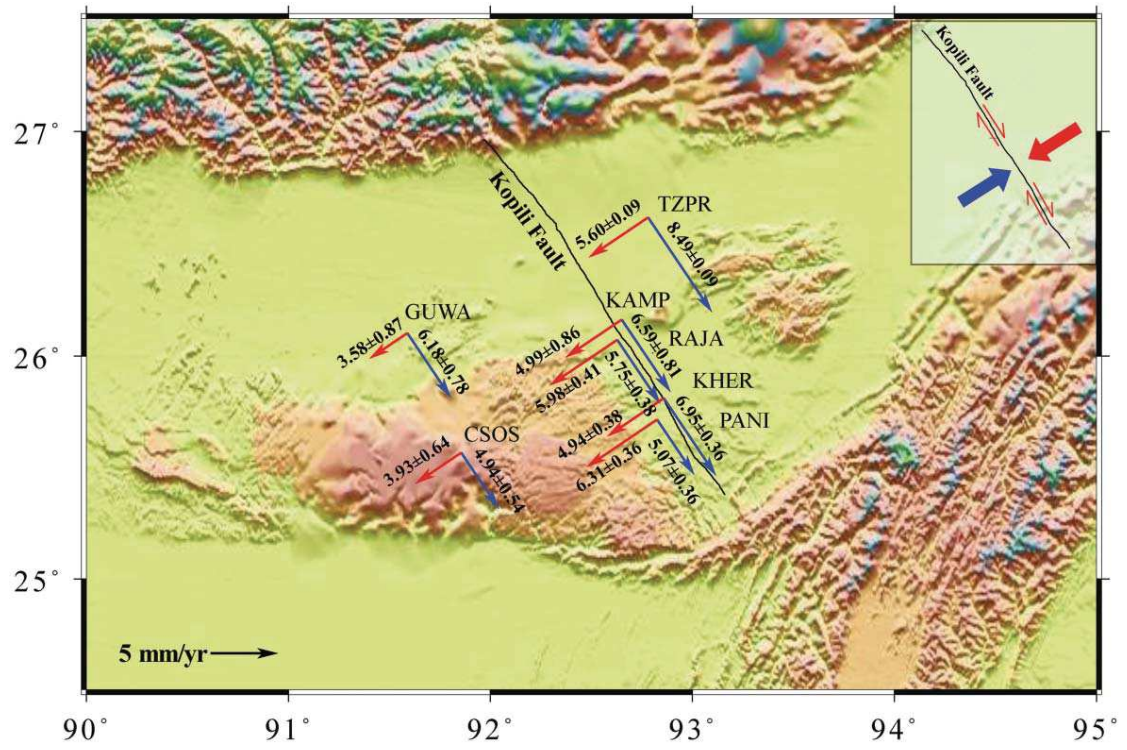

Figure 7. Velocity components resolved along strike parallel (blue arrows) and strike normal (red arrows) directions of the Kopili fault. To view this figure in colour, please see the online version of the journal.

The strike-normal velocities of the campaign sites indicate extension of ~1 mm/yr rather than compression, which may be due to the local deformation or complex geometry of the Kopili fault. According to Vernant et al. (2014), Assam valley is fragmented into the Shillong block and the Assam block along the Kopili fault and the blocks rotate clockwise relative to Indian plate. The eastern Assam block rotates slightly faster than the Shillong block resulting in ≈3 mm/yr of dextral slip across the Kopili fault zone. The four GPS campaign sites (KAMP, RAJA, KHER and PANI) are situated in the deforming zone according to the dimensions of Shillong (89°–93° E) and Assam blocks (93.5–97° E) of Vernant et al. (2014). The observed extension may be due to active shearing of Kopili fault zone. Without proper mapping and dense network of GPS observations, it is difficult to explain the observed extension. The strike-normal velocity vectors as well as the converging baselines of the permanent sites across the Kopili fault suggests that, the Kopili fault is not a pure strike slip fault rather a transpressional fault. We feel that the straight course of the Kopili fault assigned in literatures is an over-simplification. The Kopili fault zone may have a bent geometry, however, location of the bents is difficult to predict from the present study. To fully understand the site kinematics and proper delineation of the fault zone, a thorough mapping of the fault zone is required.

3.3. Elastic dislocation modelling

To invert for the slip and locking depth on the Kopili fault, we used a first-order elastic half space dislocation model described by Savage and Burford (1973) (figure 8). The model predicts the horizontal deformation and is based on the assumption of a

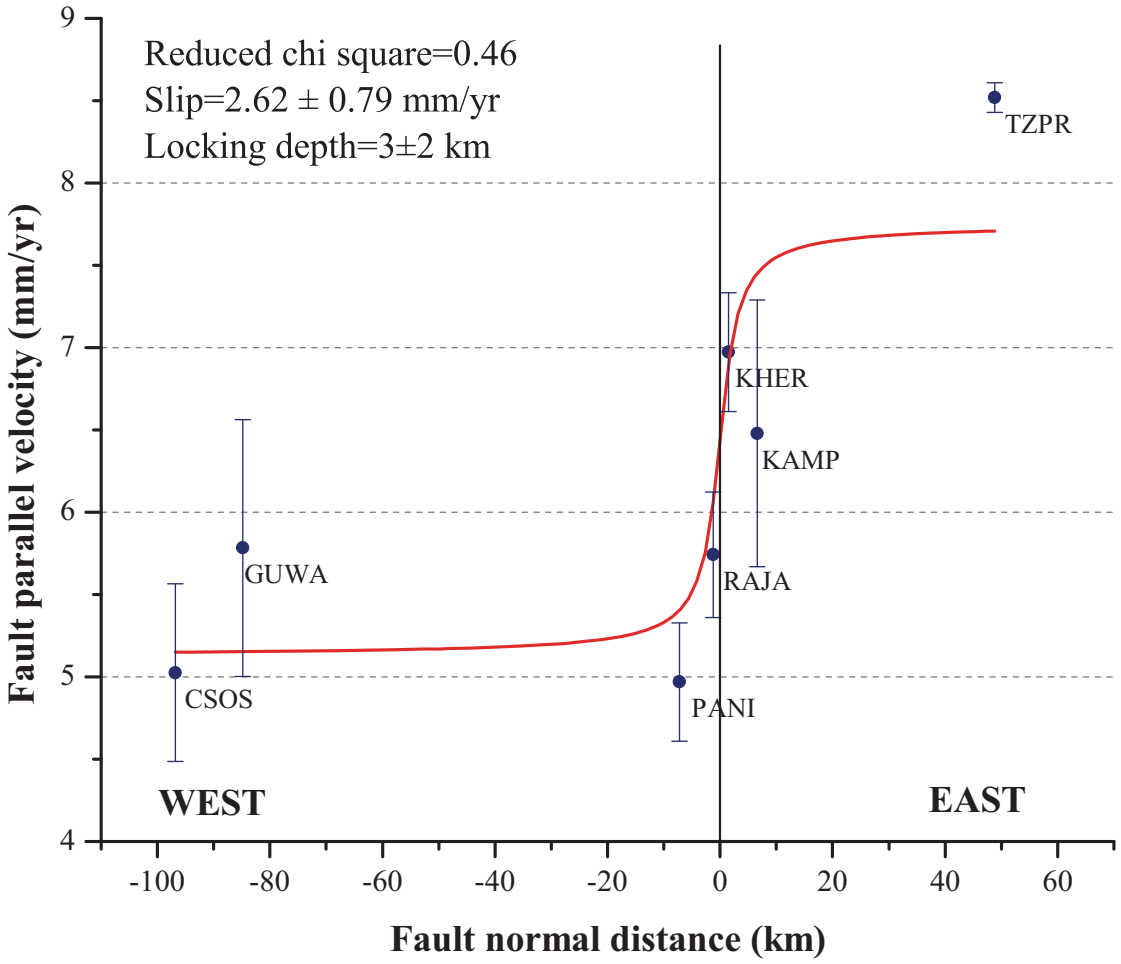

Figure 8. Elastic loading across Kopili fault. The solid vertical line is the location of the Kopili fault. The solid arctangent curve shows the best-fitting profile.

vertical dislocation of infinite length, buried in a semi-infinite elastic medium. According to this model, the fault parallel velocity $v(y)$ at a distance y perpendicular to the fault trace is given by

$$v(y) = \frac{S}{\pi}\arctan\left(\frac{y}{D}\right) \tag{1}$$

where S is the slip rate and D is the locking depth of the fault. The best-fitting elastic loading curve was obtained by non-linear least-square minimization following Levenberg–Marquardt algorithm (Pujol 2007). The best-fit elastic loading curve estimates a right lateral slip of 2.62 ± 0.79 mm/yr and a shallow locking depth (3 ± 2 km), which is consistent with the slip reported by Vernant et al. (2014). To better constrain the locking depth, we require dense GPS sites within one half of the actual locking depth (Smith-Konter et al. 2011). We have only two pairs of sites adjacent to strike of the Kopili fault on opposite sides which are not sufficient to resolve the locking depth to sufficient accuracy. Also, the current two-dimensional (2D) elastic dislocation model cannot capture completely the neotectonics of this complex fault in presence of the predominant Himalayan thrust and IBFTB subduction tectonics. Hence, it is imperative to establish more GPS sites across the fault and then invert for the fault parameters using more realistic 3D dislocation model.

3.4. Seismic hazard

Using the estimated slip rate (S) and locking depth (D), we calculated the rate of seismic moment accumulation per year ($\dot{M}$), using the expression,

$$\dot{M} = \mu \mathrm{SDL} \tag{2}$$

where $\mu = 30$ GPa is the shear modulus of the Earth and $L = 300$ km is the approximate length of the Kopili fault. Currently, seismic moment is accumulating at the rate of $\sim 70.74 \times 10^{15}$ Nm/yr, which is sufficient to source a ~5.17 Mw or greater earthquake. An order increase in moment accumulation rate (equivalent to 10 years of continuous moment accumulation) increases the Mw from 5.17 to 5.83. In the absence of intermittent earthquake, the probability of higher magnitude earthquake increases. The recent 21 September 2009 Bhutan Himalaya earthquake (Mw 6.3) and 19 August 2009 Assam valley earthquake (Mw 5.1) occurred at the northern and middle end of the Kopili fault, respectively (Kayal et al. 2010), thereby reducing the seismic moment accumulation. Therefore, on the basis of occurrence of these earthquakes and estimated slip on the Kopili fault, it can be inferred that the Kopili fault is slipping seismically in stick-slip manner and pose possible threat to the north-east India region.

4. Conclusions

We estimated the current status of deformation in the Kopili fault region of NE India using GPS data. The baseline converging rates show ~2 mm/yr E–W convergence across Kopili fault and suggest that the Kopili fault is a transpressional fault. Best-fit 2D elastic dislocation model estimates 2.62 ± 0.79 mm/yr right lateral slip of the Kopili fault at a locking depth of 3 ± 2 km. The estimated slip of 2.62 ± 0.79 mm/yr is based on the assumption of a vertical infinite strike-slip fault and is not sufficient to capture the actual deformation of this complex fault in the presence of other active faults. The slip of the Kopili fault is contributing to seismic moment accumulation ($\sim 70.74 \times 10^{15}$ Nm/yr), sufficient to drive possible future earthquakes (Mw $\geq$ 5.17). A dense GPS network and a more realistic 3D dislocation modelling are required for a complete understanding of the nature of the Kopili fault and associated seismic hazard. The current study constrains the activity of the Kopili fault in mid-Assam valley and there is a strong need for detailed investigation to resolve its activity towards the northern and southern end where it crosses MCT and Naga thrust, respectively. The deformation process in the NE India region is very complex due to the presence of collision and subduction inter-plate tectonics. The Shillong plateau bounded by the two major faults, Dauki to the South and active Kopili fault to the east, is under a threat of a medium to large earthquake(s) (Kayal et al. 2012). The Dauki fault has not slipped recently (Jade et al. 2007) and Kopili fault is slipping at ~2.6 mm/yr. To arrive at a comprehensive picture of the ongoing tectonic activity and hence seismic hazard assessment, it is essential to consider the activity of all the seismogenic sources together. With quantitative records of the past ruptures, the current rate of slip on these faults can lead to rational prediction on the occurrence of future earthquakes in this region.

Funding

This work was financially supported by the Ministry of Earth Sciences, Govt. of India vide project no. MoES/P.O.(Seismo)/1(26)/09 to Department of Physics, Tezpur University and project no. MoES/P.O.(Seismo)/GPS/48/2005 to Department of Geography, Jagiroad College, Assam, India.

References

Altamimi Z, Collilieux X, Métivier L. 2011. ITRF2008: an improved solution of the international terrestrial reference frame. J Geod. 85:457–473.

Banerjee P, Bürgmann R, Nagarajan B, Apel E. 2008. Intraplate deformation of the Indian subcontinent. Geophys Res Lett. 35:L18301.

Bendick R, Bilham R, Fielding E, Gaur VK, Hough SE, Kier G, Kulkarni MN, Martin S, Mueller K, Mukul M. 2001. The 26 January 2001 "Republic Day" earthquake, India. Seismol Res Lett. 72:328–335.

Bhattacharya PM, Majumdar RK, Kayal JR. 2002. Fractal dimension and b-value mapping in northeast India. Curr Sci. 82:1486–1491.

Bhattacharya PM, Mukhopadhyay S, Majumdar RK, Kayal JR. 2008. 3-D seismic structure of the northeast India region and its implications for local and regional tectonics. J Asian Earth Sci. 33:25–41.

Bilham R, England P. 2001. Plateau "pop-up" in the Great 1897 Assam Earthquake. Nature. 410:806–809.

Chen WP, Molnar, P. 1990. Source parameters of earthquakes and intraplate deformation beneath the Shillong plateau and northern Indo-Burma ranges. J Geophys Res. 95:12527–12552.

Chowdhury JD, Sarma I, Bora M, Banerjee P. 2005. Feasibility report on "A delineation of the seismically active Kopili fault zone of north-east India". New Delhi: DST.

Dasgupta S. 2011. Earthquake geology, geomorphology and hazard scenario in northeast India: an appraisal. In: Chakrabarti PGD, Ghosh C, editors. National workshop on earthquake risk mitigation strategy in north east. New Delhi: National Institute of Disaster Management; p. 24–39.

Dasgupta S, Mukhopadhyay M, Nandy DR. 1987. Active transverse features in the central portion of the Himalaya. Tectonophysics. 136:255–264.

Dasgupta S, Nandy DR. 1982. Seismicity and tectonics of Meghalaya plateau, NE India. Paper presented at: VIII Symposium on Earthquake Engineering; University of Roorkee, India.

DeCelles PG, Robinson DM, Zandt G. 2002. Implications of shortening in the Himalayan fold-thrust belt for uplift of the Tibetan plateau. Tectonics. 21:12–1–12-25.

Dow JM, Neilan RE, Rizos C. 2009. The international GNSS service in a changing landscape of global navigation satellite systems. J Geod. 83:191–198.

Evans P. 1964. Tectonic framework of Assam. J Geol Soc India. 5:80–96.

Herring TA. 2003. MATLAB tools for GPS time series and velocities. GPS Solut. 7:194–199.

Herring TA, King RW, McClusky SC. 2010a. Documentation of the GAMIT GPS analysis software release 10.4. Cambridge (MA): Department of Earth, and Planetary Sciences, Massachusetts Institute of Technology.

Herring TA, King RW, and McClusky SC. 2010b. GLOBK, Global Kalman filter VLBI and GPS analysis program, version 10.4. Cambridge (MA): Department of Earth, and Planetary Sciences, Massachusetts Institute of Technology.

Jade S, Mukul M, Bhattacharya A, Vijayan MSM, Jaganathan S, Kumar A, Tiwari RP, Kumar A, Kalita S, Sahu SC, et al. 2007. Estimates of interseismic deformation in northeast India from GPS measurements. Earth Planet Sci Lett. 263:221–234.

Kayal JR, Arefiev SS, Baruah S, Hazarika D, Gogoi N, Gautam JL, Baruah Santanu, Dorbath C, Tatevossian R. 2012. Large and great earthquakes in the Shillong

plateau–Assam valley area of northeast India region: pop-up and transverse tectonics. Tectonophysics. 532–535:186–192.

Kayal JR, Arefiev SS, Baruah S, Tatevossian R, Gogoi N, Sanoujam M, Gautam JL, Hazarika D, Borah D. 2010. The 2009 Bhutan and Assam felt earthquakes (Mw 6.3 and 5.1) at the Kopili fault in the northeast Himalaya region. Geomat Nat Haz Risk. 1:273–281.

Kundu B, Gahalaut VK. 2013. Tectonic geodesy revealing geodynamic complexity of the Indo-Burmese arc region, north east India. Curr Sci. 104:920–933.

Mahesh P, Catherine JK, Gahalaut VK, Kundu B, Ambikapathy A, Bansal A, Premkishore L, Narsaia M, Ghavri S, Chadha RK, et al. 2012. Rigid Indian plate: constraints from GPS measurements. Gondwana Res. 22:1068–1072.

Mitra S, Priestley K, Bhattacharyya AK, Gaur VK. 2005. Crustal structure and earthquake focal depths beneath northeastern India and southern Tibet. Geophys J Int. 160:227–248.

Mukul M, Jade S, Bhattacharyya AK, Bhusan K. 2010. Crustal shortening in convergent orogens: insights from global positioning system (GPS) measurements in northeast India. J Geol Soc India. 75:302–312.

Nandy DR. 1980. Tectonic patterns in northeastern India. Indian J Earth Sci. 7:103–107.

Nandy DR. 1981. Discussion on tectonic patterns in northeastern India. Reply. Indian J Earth Sci. 8:82–86.

Nandy DR. 2001. Geodynamics of northeastern India and the adjoining region. Calcutta: ACB Publishers.

Oldham RD. 1899. Report on the great earthquake of 12th June 1897. Geol Surv India Memoir. 29:1–379.

Pujol J. 2007. The solution of nonlinear inverse problems and the Levenberg–Marquardt method. Geophysics. 72:W1–W16.

Savage JC, Burford RO. 1973. Geodetic determination of relative plate motion in central California. J Geophys Res. 78:832–845.

Smith-Konter BR, Sandwell DT, Shearer P. 2011. Locking depths estimated from geodesy and seismology along the San Andreas fault system: implications for seismic moment release. J Geophys Res. 116:B06401.

Vernant P, Bilham R, Szeliga W, Drupka D, Kalita S, Bhattacharyya AK, Gaur VK, Pelgay P, Cattin R, Berthet T. 2014. Clockwise rotation of the Brahmaputra Valley relative to India: tectonic convergence in the eastern Himalaya, Naga hills, and Shillong plateau. J Geophys Res Solid Earth. 119:6558–6571.